Available online at www.sciencedirect.com
SCIENCE DIRECT®
Ocean Modelling 5 (2003) 219–231
Ocean Modelling
www.elsevier.com/locate/omodol

Treatment of unresolved islands and ice in wind wave models ☆

Hendrik L. Tolman *

SAIC-GSO at NOAA/NCEP/EMC Marine Modeling and Analysis Branch, 5200 Auth Road, Room 209, Camp Springs, MD 20746, USA

Received 2 April 2002; received in revised form 25 July 2002; accepted 26 July 2002

Abstract

In ocean wave prediction models, unresolved islands are a major source of (local) errors. This paper presents a method based on a technique used in the SWAN model to deal with such islands. The method is tested in the operational global WAVEWATCH III model of the National Centers for Environmental Prediction with a one year hindcast, and the results show a local but dramatic impact on model errors. An added benefit of this methodology is the possibility to model the effects of polar ice coverage on waves continuously. A simple model to continuously model ice coverage is suggested. This new ice model shows mixed results in the tests.

Keywords: Wind waves; Islands; Sea ice; Obstructions; Sub-grid numerical modeling

1. Introduction

Wind waves at the surface of the oceans are generally described with their energy or variance spectrum F, defined as a function of the spectral frequency f and direction θ. In wave models, this spectrum is then treated as a slowly varying function of the spatial coordinates $\vec{x}$ and time t. In its most general form, the evolution equation for wave spectra is given as

$$\frac{\mathrm{D}F(f,\theta;\vec{x},t)}{\mathrm{D}t} = S(f,\theta;\vec{x},t), \tag{1}$$

☆ MMAB contribution Nr. 221.

* Tel.: +1-301-763-8000x7253; fax: +1-301-763-8545.
E-mail address: hendrik.tolman@noaa.gov (H.L. Tolman).

1463-5003/03/$ - see front matter
PII: S1463-5003(02)00040-9

where the source function S represents processes such as interaction between wind and waves, wave–wave interactions, and wave energy loss due to wave breaking. Alternative descriptions in terms of wave action or with spectra as a function of wavenumber yield a similar equation.

Numerical modeling of Eq. (1) generally involves discretization of the spectral (f,θ) and physical $(\vec{x})$ spaces, while marching forward in time t. The necessary four-dimensional discretization results in the need for a trade-off between accuracy (high resolution) and economy (low resolution). In recent wave models a typical spectral resolution is 24 directions with $\Delta\theta = 15°$, and 25–35 frequencies with a constant relative increment of typically 10%. Spatial resolutions of operational models are mostly dictated by economics, and by the nominal resolutions of modelled wind fields employed to drive these models. This has lead to global wave models with a resolution of the order of 100 km, and regional models with resolutions of the order of 25 km or better.

An important consideration in determining spatial resolution is the need to properly resolve coastlines and islands. With the spatial resolutions used in global models, many island groups are not resolved at all. This in fact is a major source of errors in such models, as is illustrated in, for instance, Fig. 3 of Tolman (2001), and Fig. 8 of Tolman et al. (2002). To alleviate this problem, high resolution is needed near islands, which generally cover only a small fraction of the grid. Away from islands, the necessary wave model resolution still is dictated by the resolution of the wind. Hence, increasing resolution throughout the grid to resolve islands does not appear to be economically sound. An alternative is given in recent releases of the SWAN model (Holthuijsen et al., 2001), where unresolved obstacles are included by suppressing wave energy transport between grid points. This method so far has only been used on small scales, for instance to model breakwaters in harbors. With a similar approach the dissipative effect of unresolved islands on swell propagation in large scale models can be modelled without resorting to increased model resolution.

The present study tests sub-grid modeling of islands in the operational global wave model of National Centers for Environmental Prediction (NCEP) (see Tolman et al., 2002). Details of the methodology are given in Section 2. The use of sub-grid obstacles can furthermore be expanded to the treatment of polar ice coverage, which is usually represented by an ice concentration from analyses or models. Conventionally, grid points are (discontinuously) taken out of the wave model when a threshold concentration is reached. A new continuous method is suggested, where ice is modelled as a partial obstruction (Section 3) which scales with the ice concentration. In Section 4, results of a one year hindcast are presented. Discussion and conclusions are presented in Section 5.

2. Unresolved islands

In a numerical model, Eq. (1) is normally solved using fractional steps. Typically, one such step deals with the right hand side (sources), and one or more deal with the propagation terms of the left side. In NCEP's WAVEWATCH III models spatial propagation is treated in a separate step. The spatial propagation equation solved in this step is given as

$$\frac{\partial F}{\partial t} + \frac{\partial cF}{\partial x} = 0, \tag{2}$$

where c is the advection velocity in physical space. For simplicity, the one-dimensional version of this equation is given, and the functional dependence of F is omitted from the notation. For a given spectral component, the numerical propagation schemes as used by WAVEWATCH III can be written as

$$F_i^{n+1} = F_i^n + \frac{\Delta t}{\Delta x}[G_{i,-} - G_{i,+}]^n, \tag{3}$$

where i and n are discrete space and time counters, respectively, and where $G_{i,-}$ is the flux at the cell boundary between the grid points with counters i and $i-1$,

$$G_{i,-}^n = 0.5(c_{i-1} + c_i)F_{\mathrm{b}}^n, \tag{4}$$

where F_{b} is the spectral density at the cell boundary. The actual calculation of F_{b} determines the nature and accuracy of the numerical scheme. In WAVEWATCH III, F_{b} is calculated according to the ULTIMATE QUICKEST scheme of Leonard (1979, 1991). $G_{i,+}$ is the flux at the cell boundary between grid points i and $i+1$, defined similarly. To assure numerical conservation of energy, $G_{i+,} \equiv G_{i+1,-}$. Starting from Eq. (3), and following Holthuijsen et al. (2001), sub-grid islands and other obstacles can be modelled as physically reduced energy fluxes between cells,

$$F_i^{n+1} = F_i^n + \frac{\Delta t}{\Delta x}[\alpha_{i,-}G_{i,-} - \alpha_{i,+}G_{i,+}]^n, \tag{5}$$

where $\alpha_{i,-}$ and $\alpha_{i,+}$ are 'transparencies' of the corresponding cell boundaries, ranging from 0 (closed boundary) to 1 (no obstructions). For outflow boundaries, transparencies by definition are 1, otherwise energy will artificially accumulate in cells. For inflow boundaries, transparencies less than 1 result in elimination of obstructed energy at the cell boundary.

To simplify the maintenance and generation of grids with water depths and obstructions, the obstructions will be defined at the center of grid boxes, instead of on the cell boundaries (the latter would result in staggered grids). To assure that half the obstruction α_i for cell i occurs at the cell center, the inflow transparency becomes $0.5(1+\alpha_i)$, and the outflow transparency by definition is 1. To complete the total transparency α_i, the next cell in the flow direction will have an inflow transparency $2\alpha_i/(1+\alpha_i)$. The total transparency for the cell becomes the product of the two factors, which equals α_i. If two adjacent cells have restricted transparencies, the actual inflow transparency will become a product of the cell transparency and the transparency at the upstream cell. Assuming for simplicity that $c > 0$, this results in

$$\left.\begin{aligned} \alpha_{i,-} &= \frac{\alpha_{i-1}(1+\alpha_i)}{1+\alpha_{i-1}} \\ \alpha_{i,+} &= 1 \end{aligned}\right\}. \tag{6}$$

Generalization to arbitrary c is straightforward.

Applying this sub-grid island approach to a wave model requires the generation of bathymetry and obstruction grids. To generate such grids, a global 5′ resolution bathymetry data set was extracted from the Naval Oceanographic Office's DBDB-V database version 4.1. [1] Fig. 1 gives

[1] http://idbms.navo.navy.mil/dbdbv/dbdbv.html and http://idbms.navo.navy.mil/dbdbv/database_doc.html.

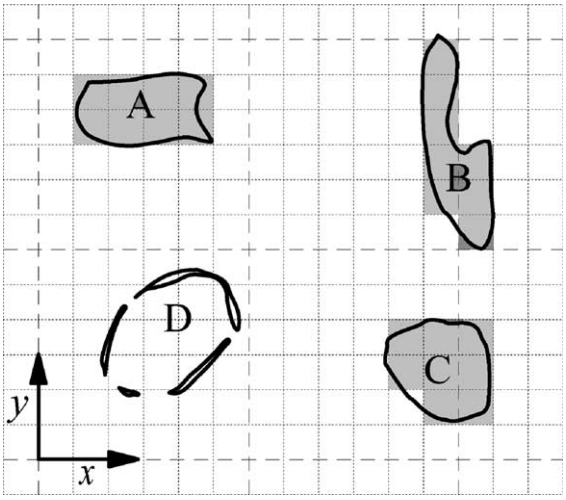

Fig. 1. Some examples to illustrate generation of obstruction grids and corresponding problems. Dotted lines are boundaries of grid cells in the high resolution grid. Dashed lines correspond to model grid. Solid lines represent coast lines of islands, and grey shading represents representation of islands in the high resolution grid.

some examples to illustrate how a wave model grid can be generate from such a high resolution or 'fine' grid, as well as problems encountered in this process.

In principle, the transparencies for a wave model grid can be determined objectively from the fine grid, as the fraction of transparent grid lines of the fine grid within the grid cell of the wave model. For island A in Fig. 1, four of the six fine grid lines in the x direction within the grid cell of the wave model are transparent, resulting in $\alpha_x = 0.66$. Similarly, $\alpha_y = 0.33$. Difficulties occur, however, with islands straddling grid cells. Island B in Fig. 1 should completely block wave propagation in x direction ($\alpha_x = 0$) for the grid line it covers in the wave model. However, with the above procedure, it results in $\alpha_x = 0.17$ and $\alpha_x = 0.5$ in two adjacent cells, and hence in a total transparency $\alpha_x = 0.08 \neq 0$. Such a situation can lead to spurious swell penetration in completely sheltered areas. Similarly, island C should result in $\alpha_x = 0.5$, but the above method results in this transparency in two adjacent cells, resulting in a net transparency of the island of $\alpha_x = 0.25$. Finally, atoll C is completely missed in the fine grid, and can therefore not result in the proper obstruction in the wave model grid when the above method is used. Additional intervention is required for many reasons, such as: (i) blocking out of unwanted parts of domains, (ii) corrections of obvious errors remaining in the database (rare but necessary), (iii) resetting transparencies for grid points adjacent to land to $\alpha = 1$, to prevent the swell energy approaching land from being suppressed in the last grid point by other than true dissipation mechanisms.

If a high resolution grid can be constructed, that properly deals with islands like D in Fig. 1, a reasonable automated grid generation algorithm can probably be designed. This would, however, require a significant development effort, which cannot be justified before this sub-grid method is proven to be effective. Therefore, the required wave model grid for the present study has been generated interactively, based on the methodology and considerations discussed above. Fig. 2 shows the resulting grid for NCEP's global wave model (e.g., Chen et al., 1999; Tolman et al., 2002). Regular land points are grey, partially obstructed points are black. Note that the latter

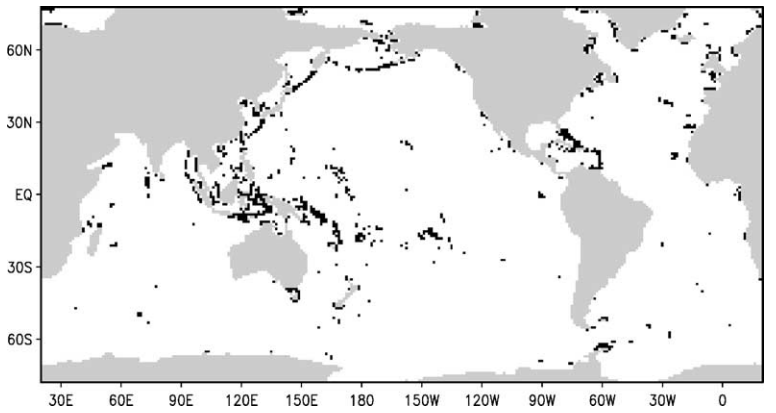

Fig. 2. Grid layout of NCEP's global wave model. Grey identifies land points, black identifies grid points with some obstruction in longitudinal or latitudinal direction ($\alpha \neq 1$).

include all partially obstructed grid points, including many which only represent minor obstructions. The figure shows that partially obstructed grid points represent many major island chains. Although the distribution of partially obstructed grid points is distinctive, the number of such grid points is small (only 3.2% of the 'sea' points in this model).

3. Ice concentrations

NCEP's operational wave models use ice concentrations from NCEP's automated passive microwave sea ice concentration analysis (Grumbine, 1996). Ice concentrations represent the fraction of sea covered with ice. Presently the ice concentration is only used to identify points as regular sea points, or as points to be taken out of the calculation completely, based on some cut-off ice concentration (presently 33%). This corresponds in practice to a discontinuous change from model points without ice, to fully ice covered grid points. The introduction of partially obstructed grid points in the wave model provides a more natural way to continuously model ice coverage.

Detailed analyses of the effects of ice floes on wave propagation have been published (e.g., Wadhams et al., 1986; Masson and LeBlond, 1989), many in Russian literature (see Lavrenov, 1998). It has been shown that wave attenuation in ice fields shows an exponential decay in space with a given length scale λ. Observed decay rates can be explained with simple scattering models of waves by individual ice floes. The amount of scattering or λ is (amongst others) a function of wave frequency, the ice floe distribution, and the ratio of wave length to ice floe length. Considering that only an ice concentration estimate is available in operational models, it is clear why advanced models for wave attenuation by ice are not yet used in ocean wave models. A simple model based on concentrations only will therefore be constructed here, based on both physical and modeling considerations.

It is assumed that wave energy will not be dissipated instantaneously when the wave field encounters ice. Instead, waves are assumed to progressively loose energy while travelling through an ice field, consistent with exponential decay behavior as mentioned above. The decay rates are

expected to be a distinct function of the size of individual ice floes (e.g., Masson and LeBlond, 1989), with larger ice floes scattering waves more efficiently, and hence resulting in larger decay rates. Since it furthermore seems natural to assume that floe sizes increase with ice concentration, it may be expected that decay rates increase strongly with ice concentration. Because the model lacks the necessary data to estimate decay rates parametrically (see above), there is no justification to go beyond a very simple model. It will be assumed that upon penetrating the ice field over a distance l_0, ice induced wave attenuation can still be neglected. Between the distances l_0 and l_n, the entire wave energy is dissipated. Lacking any solid physical considerations to choose otherwise, a simple linear decay model will be adopted.

For an ice concentration ϵ, the average distance by which the waves travel through ice per grid box scales linearly with ϵ and Δx or Δy. Applying the above described simple model locally per grid box, transparencies α become

$$\alpha_x = \begin{cases} 1 & \text{for } \epsilon\Delta x < l_0 \\ 0 & \text{for } \epsilon\Delta x > l_n \\ \dfrac{l_n - \epsilon\Delta x}{l_n - l_0} & \text{otherwise} \end{cases}, \quad \alpha_y = \begin{cases} 1 & \text{for } \epsilon\Delta y < l_0 \\ 0 & \text{for } \epsilon\Delta y > l_n \\ \dfrac{l_n - \epsilon\Delta y}{l_n - l_0} & \text{otherwise} \end{cases}. \tag{7}$$

Note that the explicit dependency of α on the grid increments Δx and Δy assures directional isotropy of the effects of ice on wave propagation, and is therefore an important aspect of this simple model.

If this simple model is applied locally per grid box in a wave model, it is imperative that $l_n < \max(\Delta x, \Delta y)$. If this condition is not met, $\max(\alpha_x, \alpha_y) > 0$ even for $\epsilon = 1$, and grid points cannot be taken out of the calculation even if fully covered by ice. The situation becomes particularly awkward when a spherical grid is used. The longitudinal increment Δx then systematically reduces to 0 approaching the poles. This can result in a situation where ice covered grid points are taken out of the calculation for lower latitudes, yet always remain in the calculation near the poles. A simple way to avoid this is to define a critical ice concentrations $\epsilon_{c,0}$ and $\epsilon_{c,n}$ defining initial and total impediment of wave propagation, and then define l_0 and l_n, locally as

$$l_0 = \epsilon_{c,0} \min(\Delta x, \Delta y), \quad l_n = \epsilon_{c,n} \min(\Delta x, \Delta y). \tag{8}$$

Having no objective guidance for realistic values for the critical ice concentrations, they will be set to $\epsilon_{c,0} = 0.25$ and $\epsilon_{c,n} = 0.75$ in the tests, around the previous cut-off concentration $\epsilon_c = 0.33$. The final continuous ice model is then obtained by calculating length scales from local ice concentrations using Eq. (8), and substituting these in Eq. (7) to obtain cell transparencies.

The obstructions provided by ice are combined with the obstructions provided by unresolved islands by using the product of the corresponding cell transparencies. Note that unlike island obstructions, ice obstructions are regularly updated in the model.

4. Model results

To test the concepts of sub-grid modeling of islands and ice in wave models, a one year hindcast run is made with NCEP's global wave model (see Fig. 2). The hindcast period covers March 2000 through February 2001. The wind fields used consist of alternating analyses and 3 h forecasts

from NCEP's Global Data Assimilation (GDAS) and Medium Range Forecast (MRF) systems (e.g., Caplan et al., 1997). The spectral resolution of these wind fields is T170. Validation of the hindcast runs is performed with buoy data and ERS-2 altimeter data, as described in Tolman et al. (2002).

These test runs are a part of a systematic effort aimed at validating and testing a new version of the operational WAVEWATCH III models at NCEP (Tolman, 2002c). The control calculations are therefore not performed with the presently operational version 1.18 of WAVEWATCH III, but with a newer version. This 'baseline version' differs from version 1.18 in several ways: (i) The code is rewritten in FORTRAN 90 to simplify maintenance. (ii) The time integration of the source term is made forward in time cf. Hargreaves and Annan (2001), and the setting of numerical parameters in the dynamical integration scheme are slightly modified to make the integration smoother as well more responsive, (iii) The GSE alleviation of Booij and Holthuijsen (1987) is replaced by the averaging method of Tolman (2001, 2002a). Although these changes have distinct positive impact on model economy and maintenance, their impact on model results are small (see Tolman, 2002b). In the present context, the newer baseline model will be denoted as the 'old' model, that is, the model without the changes suggested here. This model augmented with the sub-grid islands and ice is similarly denoted as the 'new' model.

It is expected that effects of the sub-grid treatment of islands and ice floes are mostly confined to regions where this sub-grid treatment is activated. Buoy observations are generally not properly situated to capture these effects. ERS-2 altimeter data, however, provide balanced global coverage, including areas affected by the new sub-grid approaches. The model results against altimeter data will therefore be presented and discussed first. Only mean observed significant wave heights ($H_s = 4\sqrt{\int\int F(f,\theta)\,\mathrm{d}f\,\mathrm{d}\theta}$), their biases and standard deviation (std) errors will be considered.

Fig. 3 shows mean altimeter wave heights and biases for the old and new models. Both models show small biases compared to the mean wave heights. The bias patterns are nevertheless distinctly different. The old model (Fig. 3b) shows distinct positive biases for virtually all unresolved island groups as identified in Fig. 2. The positive bias of many such island groups manifests as a "bull's eye" near their location, and can in the tropics be as large as 50% of the mean observed H_s. Particularly distinct is the effect of the Tuamotu Archipelago around 20° S 140° W (Figs. 2 and 3b). The blocking effect of these islands is even obvious in the mean altimeter observations (Fig. 3a). In the new model virtually every positive bias area corresponding to unresolved islands has been eliminated or is greatly reduced (Fig. 3c). The bull's eye pattern of positive biases in the tropics has been replaced by a moderate but systematic negative bias. The differences in bias patterns between the old and new models can be as large as 0.6 m, with an absolute improvement in bias as large as 0.5 m. The bias patterns at high latitudes are largely unchanged, with slightly increased negative coastal biases in the northern hemisphere.

Fig. 4 presents the random part of the wave height errors of the old and new model, as well as their difference. The impact of the sub-grid representation of the islands is less dramatic than with the biases (differences in std of up to 0.1 m and 20%). Nevertheless, the impact of the sub-grid island representation on the random model errors is also positive and notable for every major island group, and limited to the direct vicinity of such groups. The impact of the sub-grid island representation on the random part of the error is due to the fact that the swells that are influenced occur as specific events. Hence, the bias reduction near islands varies in time, and therefore has an impact on both biases and random errors.

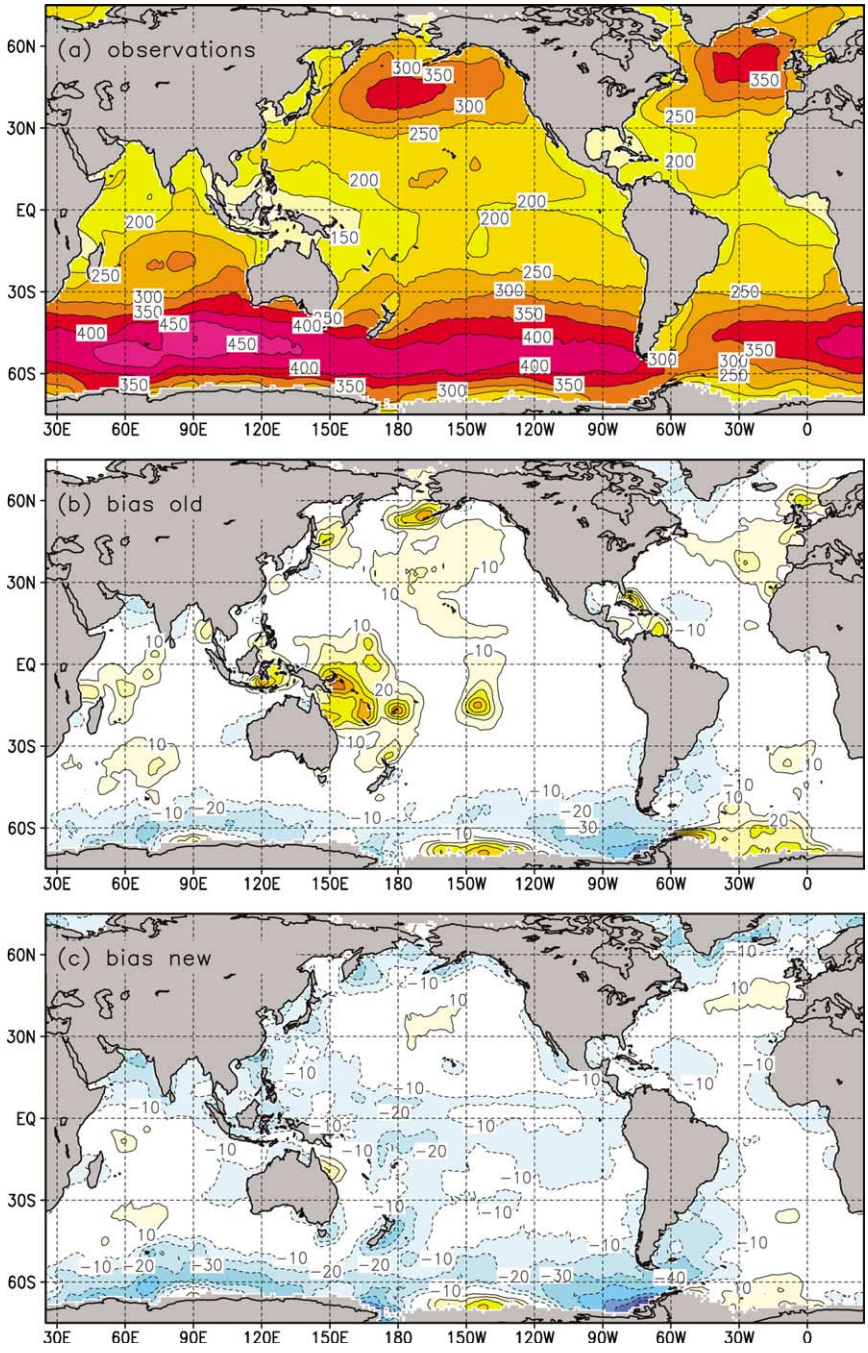

Fig. 3. Mean observed wave height H_s and model biases ΔH_s in cm from ERS-2 altimeter. Dark grey identifies lack of data (land and ice). Contours at 50 and 10 cm intervals, respectively. Dotted contours correspond to negative values, $\Delta H_s = 0$ contour not shown. $H_s > 3$ m and negative ΔH_s shaded light grey in black and white version. (a) Observed wave height, (b) old model bias, (c) new model bias.

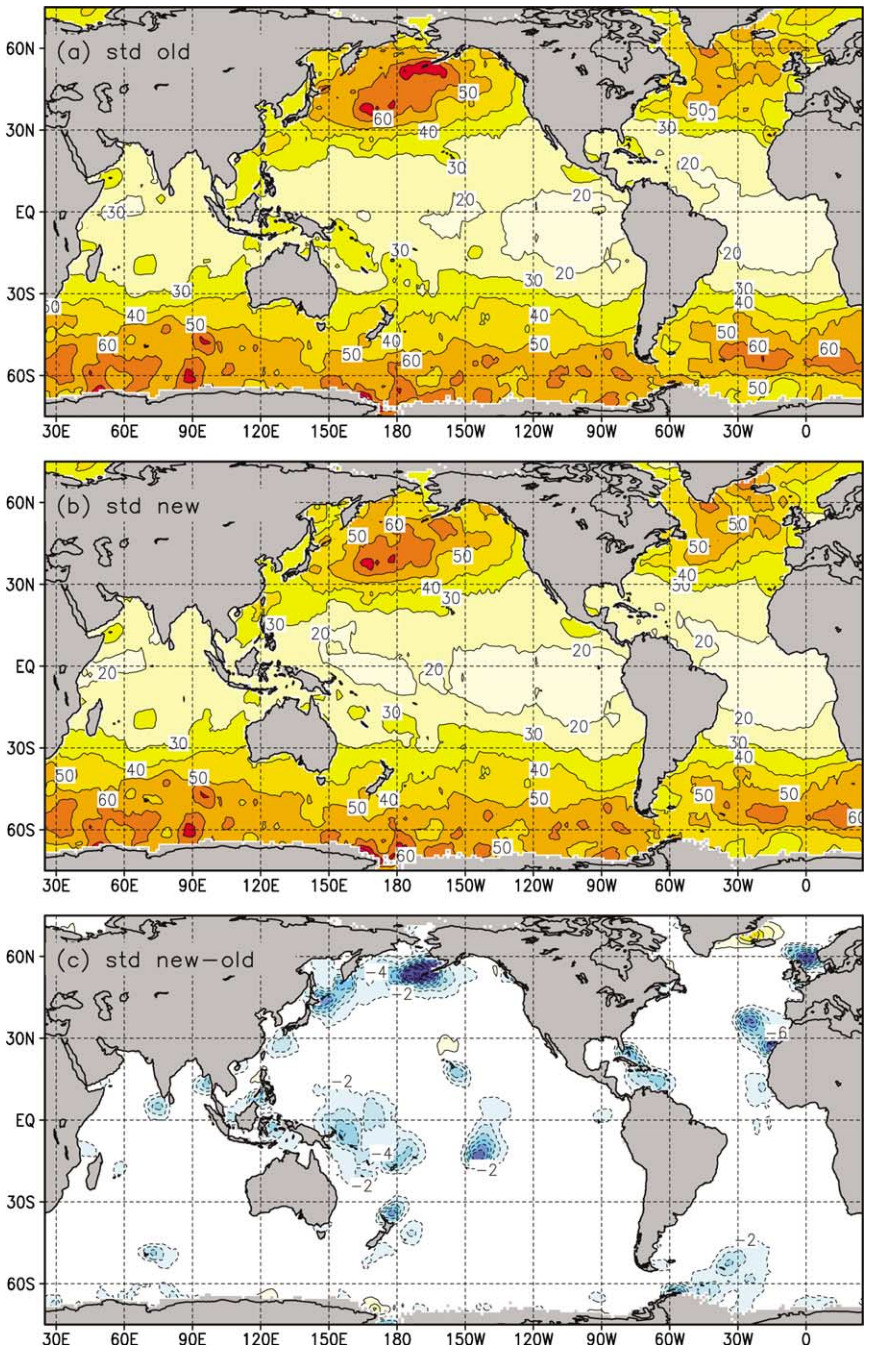

Fig. 4. Wave height std error in cm of models against ERS-2 data. Dark grey identifies lack of data. Dotted contours correspond to negative values, $\Delta\text{std} = 0$ contour not shown, std > 50 cm and negative differences shaded light grey in black and white version. (a,b) Old and new model, contours at 10 cm intervals. (c) Difference, contours at 2 cm intervals.

Effects of the continuous ice treatment are expected to be limited to ice covered areas, typically above 60° N and 60° S. In such areas, the impact of continuous ice treatment on biases (Fig. 3b and c) and random errors (Fig. 4c) are alternately positive and negative. With a slightly more negative impact in the northern hemisphere.

The impact of the modifications to the model are large but local. This implies that the effect on bulk model statistics against altimeter or buoy data is not expected to be large. Indeed, of all conventional statistics, only bulk biases show a moderate downward shift of about 0.10 m (see Tolman, 2002b, figures not presented here). Nevertheless, time series for selected buoys and selected periods do show a distinct impact of the sub-grid representation of islands. This is illustrated in Fig. 5 with three selected time series.

Buoy 22001 in the East China sea is sheltered by the Ryukyu Islands. The top panel of Fig. 5 shows time series for this buoy for July 2000. The model without sub-grid island representation (dotted or red line) systematically overestimates observed wave conditions (+), in particular for low, swell dominated, wave heights. The model with sub-grid islands (solid or green lines) pro-

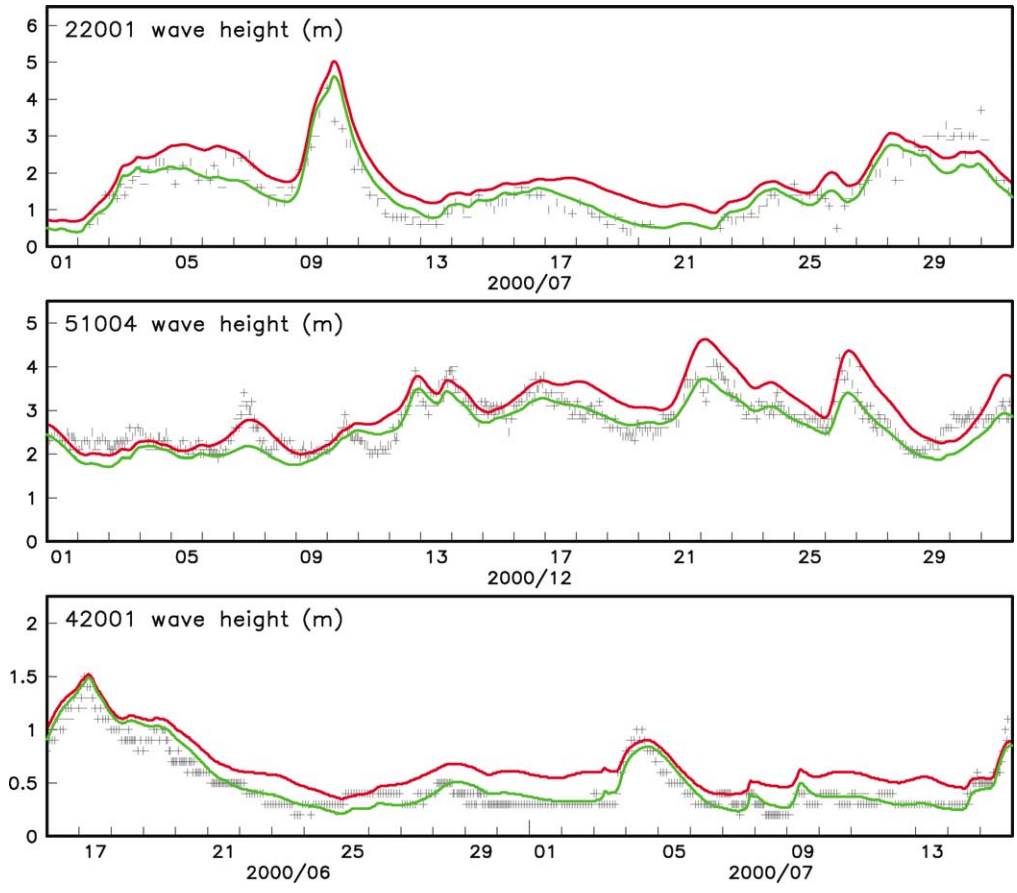

Fig. 5. Time series of wave height H_s observed at buoys (+), from the old model (dashed or red lines) and from the new model (solid or green lines) for selected buoys and periods (see Tolman et al., 2002, Fig. 1).

duces systematically lower wave heights, generally in better agreement with observations (+). These observations are fairly representative for the entire period for which data are available (through September 2000).

Systematic impact of sub-grid modeling of islands is also found for buoy locations around Hawaii, where, depending on dominant wave directions, one or more of the four buoys 51001 through 51004 are partially sheltered. The most dramatic impact is found here for the buoys south of Hawaii in the Northern Hemisphere winter, when the dominant waves consist of large swells coming from storm tracks just north of Hawaii. This is illustrated in the middle panel of Fig. 5 for buoy 51004 in December 2000. As for buoy 22001, the sub-grid representation of islands dramatically improves model behavior.

Somewhat surprisingly, the model shows a notable impact of the sub-grid modeling for the buoys in the Gulf of Mexico for extremely benign summer conditions. This is illustrated in the bottom panel of Fig. 5 with a month of model results and data from buoy 42001. The overestimation of high wave heights by the old model can be attributed to spurious swell propagation through the Straits of Florida. In the new model, these Straights are properly blocked by the Bahamas. This model behavior is only observed in the summer.

Finally, model economy is an important aspect of operational modeling. The new model proved about 10% more expensive to run than the old model, which is well within the constraints imposed by the operational environment at NCEP. About two thirds of the increase in computational time can be attributed to the addition of the cell transparencies in the calculation. The remaining one third can be attributed to the fact that the continuous ice treatment removes less ice covered points from the calculation than the old discontinuous approach.

5. Discussion and conclusions

In the present paper a sub-grid treatment of islands and partial ice coverage for wind wave models is suggested, based on a sub-grid obstruction approach used in the SWAN model (Holthuijsen et al., 2001). The corresponding obstructions are modelled as partially transparent cell boundaries in a general flux description of fairly arbitrary numerical schemes. To represent unresolved islands in this way, a map of cell transparencies needs to be constructed (Fig. 2). Although this is labor intensive, it has to be performed only once. After this, the increase in model run time is expected to be modest (7% in the present tests). Obstruction related to partial ice coverage are calculated objectively and dynamically from ice concentrations, using a newly proposed model.

The sub-grid approaches to islands and ice are tested with a one year hindcast run with NCEP's operational global wave model, for the period of March 2000 through February 2001. The models are validated using ERS-2 altimeter and buoy data. Validation with altimeter data shows that the sub-grid island approach has a local but massive impact on biases (Fig. 3b and c), and a more moderate but systematically positive impact on random errors (Fig. 4c). For islands groups like the Tuamotu Archipelago, this leads to a reduction of the overall rms wave height error of well over 50% (combined information of Figs. 3 and 4, or Tolman, 2002c). Most buoy locations are not conducive to illustrating the effect of sub-grid island modeling, as most are not sheltered

(mostly by design). Nevertheless, distinct positive impact can be found for selected buoys in selected seasons (Fig. 5).

One of the few remaining anomalous positive biases is found in the new model off the north east coast of Australia, over the great barrier reef (Fig. 3c). This is at least partially due to the fact that the minimum allowed water depth in this model is set to 25 m, not doing justice to the locally extremely shallow water on the reefs, and the accompanying wave attenuation as documented by Hardy and Young (1996). If such reefs are not properly resolved, they could also be modelled as partial sub-grid obstructions (Hardy et al., 2000). This possibility has not been investigated here, but deserves attention.

The continuous ice treatment has alternately positive and negative impacts in NCEP's global model. It should be noted, that similar tests with NCEP's regional Alaskan Waters model showed a clear positive impact of the continuous ice treatment (Tolman, 2002b). The present continuous ice treatment in essence is a "poor man's approach", because only ice concentrations are operationally available. As discussed in Section 3, proper treatment of ice in a wave model will require more detailed ice information. Until this is available, major improvement cannot be expected. It might be possible to improve the present ice model by subjective tuning. However, due to the limited physical basis of the model, such tuning indeed is subjective at best. The sub-grid ice approach can be introduced in the model without additional computational effort, considering that the underlying modeling of obstructions is fully justified by the treatment of islands. On its own merits, it remains to be seen that its introduction could be justified.

The introduction of sub-grid islands has replaced a bull's eye bias pattern with systematic negative biases in the tropics. This appears to indicate that swells in this model are attenuated too much. This has been suggested by others, for instance by Wingeart et al. (2001). This behavior, which can be observed more clearly when unresolved islands are accounted for, appears to be caused by limitations to the source terms as presently used in the model (Tolman, 2002b).

Acknowledgements

The author would like to thank D.B. Rao, Bob Grumbine, Y.Y. Chao, and the anonymous reviewers for their comments on early drafts of this paper. The present study was partially supported by funding from the NOAA High Performance Computing and Communication (HPCC) office.

References

Booij, N., Holthuijsen, L.H., 1987. Propagation of ocean waves in discrete spectral wave models. Journal of Computational Physics 68, 307–326.

Caplan, P., Derber, J., Gemmill, W., Hong, S.-Y., Pan, H.-L., Parish, D., 1997. Changes to the 1995 NCEP operational medium-range forecast model analysis/forecast system. Weather and Forecasting 4, 335–343.

Chen, H.S., Burroughs, L.D., Tolman, H.L., 1999. Ocean surface waves. Technical Procedures Bulletin 453, NOAA/NWS, http://polar.ncep.noaa.gov/omb/tpbs/nww3tpb/nww3tpb.html.

Grumbine, R.W., 1996. Automated passive microwave sea ice concentration analysis at NCEP. Tech. Note 120, NOAA/NWS/NCEP/OMB, 13 pp.

Hardy, T.A., Young, I.R., 1996. Field study of wave attenuation on an offshore coral reef. Journal of Geophysical Research 101, 14,311–14,326.

Hardy, T.A., Mason, L.B., McConochie, J.D., 2000. A wave model for the Great Barrier Reef. Ocean Engineering 28, 45–70.

Hargreaves, J.C., Annan, J.D., 2001. Comments on improvement of the short fetch behavior in the WAM model. Journal of Atmospheric and Oceanic Technology 18, 711–715.

Holthuijsen, L.H., Booij, N., Ris, R.C., Haagsma, I.G., Kieftenburg, A.T.M.M., Kriezi, E.E., 2001. SWAN Cycle III version 40.11 user manual. Delft University of Technology, Department of Civil Engineering, P.O. Box 5048, 2600 GA Delft, The Netherlands. See http://swan.ct.tudelft.nl.

Lavrenov, I.G., 1998. Mathematical modelling of wind waves in spatially non-homogeneous ocean. Hidrometeoizdat, St. Petersburg, Russia, 499 pp. (in Russian).

Leonard, B.P., 1979. A stable and accurate convective modelling procedure based on quadratic upstream interpolation. Computational Methods in Applied Mechanical Engineering 18, 59–98.

Leonard, B.P., 1991. The ULTIMATE conservative difference scheme applied to unsteady one-dimensional advection. Computational Methods in Applied Mechanical Engineering 88, 17–74.

Masson, D., LeBlond, P.H., 1989. Spectral evolution of wind-generated surface gravity waves in a dispersed ice field. Journal of Fluid Mechanics 202, 43–81.

Tolman, H.L., 2001. Improving propagation in ocean wave models. In: Edge, B.L., Hemsley, J.M. (Eds.), Ocean Wave Measurement and Analysis. ASCE, pp. 507–516.

Tolman, H.L., 2002a. Alleviating the garden sprinkler effect in wind wave models. Ocean Modelling 4, 269–289.

Tolman, H.L., 2002b. Testing of WAVEWATCH III version 2.22 in NCEP's NWW3 ocean wave model suite. Tech. Note 214, NOAA/NWS/NCEP/OMB, 99 pp.

Tolman, H.L., 2002c. User manual and system documentation of WAVEWATCH III version 2.22. Tech. Note 222, NOAA/NWS/NCEP/OMB, 133 pp. (DRAFT).

Tolman, H.L., Balasubramaniyan, B., Burroughs, L.D., Chalikov, D.V., Chao, Y.Y., Chen, H.S., Gerald, V.M., 2002. Development and implementation of wind generated ocean surface wave models at NCEP. Weather and Forecasting 17, 311–333.

Wadhams, P., Squire, V.A., Ewing, J.A., Pascal, R.W., 1986. The effect of the marginal ice zone on the directional wave spectrum of the ocean. Journal of Physical Oceanography 16, 358–376.

Wingeart, K.M., O'Reilly, W.C., Herbers, T.H.C., Wittmann, P.A., Jenssen, R.E., Tolman, H.L., 2001. Validation of operational global wave prediction models with spectral buoy data. In: Edge, B.L., Hemsley, J.M. (Eds.), Ocean Wave Measurement and Analysis. ASCE, pp. 590–599.